Available online at www.sciencedirect.com

ScienceDirect

International Journal of Solids and Structures 45 (2008) 908–920

INTERNATIONAL JOURNAL OF SOLIDS AND STRUCTURES

www.elsevier.com/locate/ijsolstr

Elastic characterization of orthotropic plates of any shape via static testing

Luigi Bruno *, Giuseppina Felice [1], Leonardo Pagnotta [2], Andrea Poggialini [3], Giambattista Stigliano [1]

Department of Mechanical Engineering, University of Calabria, P. Bucci Cubo 44C, Italy

Received 28 May 2007; received in revised form 10 September 2007
Available online 29 September 2007

Abstract

The paper presents an inverse procedure for identifying elastic properties of isotropic or orthotropic materials from the full-field measurement of the surface displacements of plates under flexural loading configurations. The procedure is based on a numerical–experimental optimisation process which minimizes an error function defined by subtracting the experimental data from the outputs of the numerical analysis. In each iteration the optimisation process updates the values of the elastic constants in a finite element model of the specimen used in the experimental tests. The unknown parameters are simultaneously identified by a single test and without damaging the structural integrity of the specimen. The possibility of using the methodology for characterizing any-shaped plates was investigated. The applicability and the robustness of the procedure were carried out on aluminum and unidirectional Graphite/PEEK laminate specimens. Phase-shifting speckle interferometry was employed to detect the out-of-plane displacement field of a portion of the observed surface of the specimen.

Keywords: Isotropic materials; Orthotropic materials; Elastic constants; Speckle interferometry; Finite element analysis (FEA); Genetic algorithms; Non-destructive testing (NDT)

1. Introduction

The knowledge of the elastic properties of materials is very important for both structural design and engineering applications and the possibility to measure them, fast and accurately and during the production process, could be a valid improvement for quality control (Gibson, 1994). Because of such importance, it is not

* Corresponding author. Tel.: +39 0984494839; fax: +39 0984494673.
E-mail addresses: bruno@unical.it (L. Bruno), felice@unical.it (G. Felice), pagnotta@unical.it (L. Pagnotta), poggialini@unical.it (A. Poggialini), stigliano@unical.it (G. Stigliano).
[1] Tel.: +39 0984494698; fax: +39 0984494673.
[2] Tel.: +39 0984494837; fax: +39 0984494673.
[3] Tel.: +39 0984494836; fax: +39 0984494673.

0020-7683/$ - see front matter
doi:10.1016/j.ijsolstr.2007.09.017

surprising the great number of methodologies developed and presented in the scientific literature, hence, still today, the argument gives rise to a wide interest among the researchers, especially in the context of the development of new and more complex materials, for which the classical methods of characterization appear slow, expensive and not always suitable.

When thin orthotropic materials, like rolled metal sheets or long-fibre reinforced composites, are investigated, only the four independent in-plane elastic constants have to be determined (i.e. longitudinal and transverse Young's moduli E_1 and E_2, the major Poisson's ratio v_{12} and the in-plane shear modulus G_{12}, where subscripts 1 and 2 refer to the longitudinal and transverse material symmetry axes, respectively). The approaches based on the wave propagation measurement, vibrational tests or static tests were proposed for the measurement of these elastic parameters.

In regard to the first approach, ultrasonic wave-speed measurement method is one of the most commonly used; through-transmission measuring as well as single-sided measurements are reported in literature (Prabhakaran et al., 2005). By knowing the dimensions and density of the samples and the transit time for longitudinal and transversal ultrasonic waves it is possible to evaluate Young's and shear moduli of the material and, by suitable procedures, the principal Poisson's ratio. The ultrasonic measurement techniques are not particularly straightforward, consequently the diffusion of these are limited to the research contexts, while they are hardly used for routine measurement.

Vibrational methods consist in exciting a specimen by mechanical vibration in one or more resonant sonic and/or ultrasonic modes. By the vibrational mode, frequency, dimensions and mass of the specimen it is possible to evaluate the elastic constants of the material. Recently, a great number of numerical–experimental resonant methods for the identification of the elastic properties of orthotropic specimens have been proposed. Even if a method for the direct determination of the flexural stiffness is available (Grédiac and Paris, 1996), the elastic identification is usually carried out by inverse procedures, in which the unknown material parameters are updated in a numerical or analytical model until the computed natural frequencies match the experimental observations with a fixed accuracy (a good number of references can be found in Maletta and Pagnotta (2004)). In principle, this approach makes it possible to identify all the elastic properties simultaneously from a single experiment and without damaging the specimen. On the other hand, since in dynamic regime the strain level is very low, the non-linear response of the material cannot be detected and identified.

Static (or quasi-static) methods are generally based on direct measurement of strain components and calculation (by measuring loads and geometry) of stress components during mechanical tests (tensile, compressive, flexural, torsional, etc.). Young's and shear moduli are determined from the slope of the linear region of the stress–strain curve, while Poisson's ratio is determined from the ratio between transverse and longitudinal strains (Carlsson and Pipes, 1997). A simple test procedure consists in performing on three strain-gauged specimens a tensile test, by orienting their principal axis at 0°, 45°, and 90° with respect to the loading direction. The analysis of the results obtained by testing the 0° and 90° specimens provides E_1, E_2, v_{12}, and v_{21}, while G_{12} is obtained by the 45° specimen. Unfortunately, the measurement of G_{12} is not easy and accurate as for the other parameters, this limited applicability encouraged the development of several methods for the identification of the shear modulus (rail shear, picture-frame shear, off-axis tensile shear and Iosipescu shear tests are, only, some examples).

Consequently the development of methodologies using a single specimen for measuring all the in-plane elastic constants could result very advantageous. Orthotropic half-plane specimens were proposed in Prabhakaran and Chermahini (1984), for which an analytical solution for the strain and stress fields exists, consequently pointwise measurement with strain gauges can lead to the determination of the unknown parameters. When no analytical solution is available, inverse procedures based on updating the finite element models have been developed, either in the case of a reduced number of measurements (Wang and Kam, 2000) or in the case of whole-field data. This last case could occur when data (strain or displacement fields) are measured onto the surface of the specimen with an optical method. Several types of specimen and tests were used in the papers found in the literature on the subject: open-hole uniaxial tensile tests (Molimard et al., 2005), in-plane loaded rectangular plate (Genovese et al., 2004), circular disk under diametrical compression (Wang et al., 2005; Hild and Roux, 2006), cruciform perforated specimens under biaxial tests (Lecompte et al., 2007), through hole biaxially loaded plate (Cardénas-Garcia et al., 2005).

However, the idea of determining the elastic constants of a material by the displacement fields undergone from some kind of specimen was well exploited in the past. Starting from the pioneers (Cornu, 1869; Timoshenko and Goodier, 1970), many authors, encouraged by the diffusion of the coherent light sources, developed a large number of static (Jones and Bijl, 1974; Archbold et al., 1978; Zhu, 1996; Ganesian, 1989; Grédiac and Vautrin, 1993; Gascon and Salazar, 1996; Furgiuele et al., 1997; Apalkov et al., 1999; Bruno et al., 2002a,b, 2006a,b; Bruno and Poggialini, 2005; Grédiac et al., 2006) or dynamic techniques (Fällström and Jonsson, 1991; Fällström et al., 1996; Grédiac et al., 1998; Gaul et al., 1999).

Recently, an inverse method was developed by the authors of this paper with the aim of identifying all the four engineering constants from the measurement of displacement field of a single square plate transversally loaded. Theoretical aspects of the methodology and numerical simulations for testing the accuracy and sensitivity of the method were presented by Pagnotta (2006) and Pagnotta and Stigliano (2006).

In the present paper the feasibility of testing plates of generic form was investigated, the results of the experimental assessment of the methodology are reported and discussed. The displacement fields were measured with a speckle interferometer based on Michelson design. To verify the robustness and the repeatability of the procedure, two plates were analysed: a square unidirectional Graphite/PEEK and an aluminum plate with a generic shape. The results were compared with reference values obtained by other techniques.

2. Identification of the engineering constants by updating a finite element model

When a body is loaded, each point undergoes a displacement whose amplitude depends on: the entity of the load, the coordinates of the point, the constraints and the geometry of the body and, obviously, the elastic properties of the material. If the analytical solution of the adopted loading configuration is available the elastic properties of the material could be determined by measuring the displacement fields, provided that the applied loads are previously measured or properly imposed. On the contrary if a reliable theoretical solution does not exist, a numerical solution becomes necessary. Inverse procedures based on the updating of numerical models could be suitable for this purpose.

Generally, when this type of approach is used, the mechanical response of a model of the specimen under test is correlated with the experimental observations performed on the real specimen. The unknown parameters of the material in the numerical model are updated until the mechanical behaviour matches the experimental observations as closely as possible. The values of the parameters used in the numerical model in the last computation are the results of the characterization procedure and they yield the elastic properties of the specimen. In principle, this approach makes it possible to identify all the elastic properties simultaneously from a single experiment and without damaging the structure.

Recently, a procedure following this approach was proposed by Pagnotta and Stigliano (2006). Such a procedure combines finite element analyses and genetic algorithms to identify the elastic properties of isotropic or anisotropic materials by the full-field measurement of the surface displacements of a square plate transversally loaded. A real-coded adaptive range genetic algorithm updates the elastic constant values in a finite element model, so that the outputs from the numerical analysis fit the experimental data.

A scheme of the inverse procedure is reported in Fig. 1. The first step of the genetic algorithm is the creation of a population of individuals (initial population) chosen randomly from a set of potential solutions of the problem. Single individual, formed by two (isotropic material) or four (orthotropic material) elastic constants, is subjected to the evaluation based on the following fitness function:

$$\varphi = \sum_{i=1}^{n} |w_i^{\mathrm{n}} - w_i^{\mathrm{e}}|, \tag{1}$$

which is calculated by summing the absolute value of the difference calculated between the numerical w_i^{n} and the experimental w_i^{e} out-of-plane displacements. The parameter n represents the total number of the data acquired experimentally. Then, a selection process allows to discard those individuals of lowest fitness in order to create a new population which combines the desirable characteristics of the old population. The new population replaces the old one and the process restarts. New generations are created through the genetic manipu-

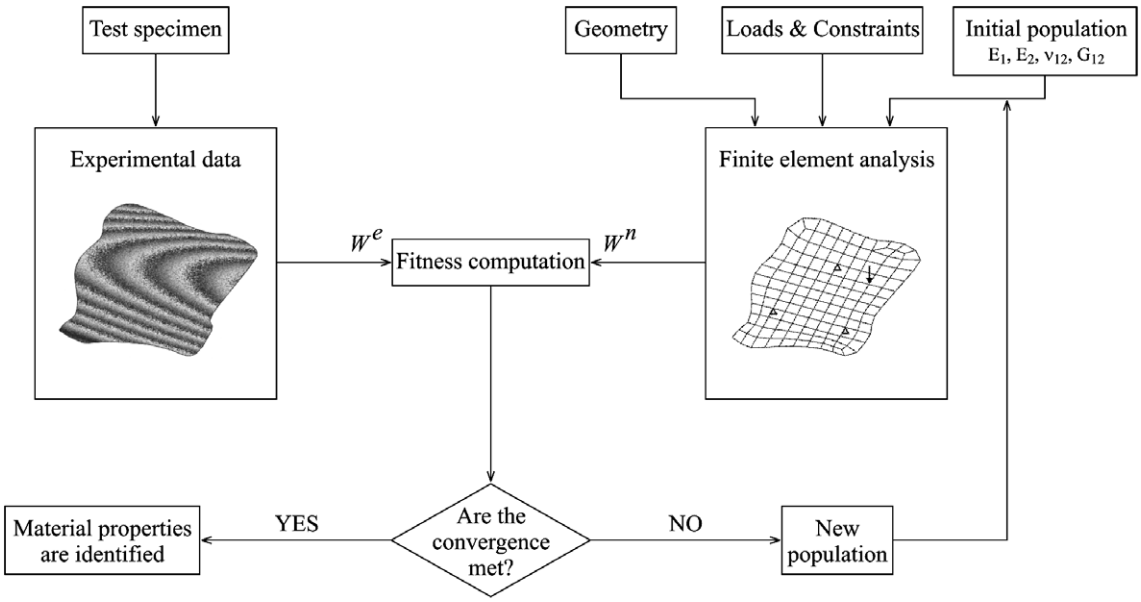

Fig. 1. Flow chart for optimal design by genetic algorithm.

lation, and this iterative process is repeated for a fixed number of generations or for a fixed number of analyses, until there is no improvement in the best solution.

The effectiveness and the robustness of the procedure with respect to the effects of measurement noise were tested by means of several numerical simulations.

The major peculiarity (and strength) of the genetic algorithms consists in the capability of simultaneous identification of the elastic constants, without paying any particular attention to the choice of the initial guess point, in fact they represent a valid tool to obtain solution even if the domain has many minimums. This situation could take place when the fitness of orthotropic material must be minimized, which never occurs for the isotropic material (in this case, only a minimum is available, hence any optimisation methodology could be adopted).

In this paper, the feasibility of applying the proposed procedure to plates of generic shape was investigated.

3. Optimisation of the loading configuration

As shown in Fig. 1, the inverse procedure implies essentially two steps: the experimental measurements and the application of the genetic algorithm. The experimental step requires the measurements of the dimensions of the plate, of the applied load and of the displacement field. Such data are necessary for the construction of the finite element model and for the numerical identification procedure, which starts in the second step.

Only a portion of the displacement field is suitable for the identification process, and, also, a single component of the displacement field is enough. The component of the displacement to be chosen depends on its sensitivity to the elastic properties and to the load variations.

In principle, any of the several full-field techniques dedicated to displacement measurement (i.e. speckle photography, speckle interferometry, geometric moiré, moiré interferometry, holographic interferometry, digital image correlation, grid methods, etc.) could be used. However, among these techniques, interferometric methods have higher sensitivities and then appear more appropriate for composite material characterization.

Full-field measurement methods provide an amount of information much greater than that required for determining the elastic constants. Hence the elastic characterization problem becomes an over-determined inverse problem and, if it turns out well-constrained, it can provide good results, thanks to the capability of this type of problems of reducing the influence of the measurement errors. Then, great care needs to be taken in choosing how to load and constrain the plate in such a way as the resulting displacement field

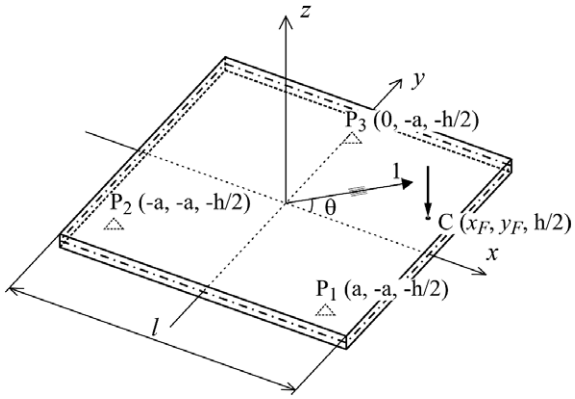

Fig. 2. The loading configuration used to identify by the correlation index the best location for the load.

contains enough information to determine all the unknown parameters, quickly and straightforwardly. Pagnotta (2006) proposed a numerical procedure for optimising the loading and constraining conditions of the specimen. Basically, the procedure consists in determining the conditions which minimize the "correlation index" i_c. This index represents the degree of statistical correlation between the variation of the displacement fields due to a variation of the elastic constants and its absolute value is, by definition, less than or equal to unity. In the case of isotropic plates the correlation index is the same of correlation coefficient, while for orthotropic plates the correlation index is the mean of the absolute values of the correlation coefficients.

As reported by Pagnotta and Stigliano (2006), such a procedure was used to identify a loading and constraining configuration, practical and simple to replicate in lab, by which the elastic constants of a square plate specimen are identified by measuring the out-of-plane component (normal to the surface) of the displacement field. The square plate was assumed simple supported on three points P_1, P_2, and P_3 lying on the corners of an isosceles triangle, as reported in Fig. 2. By considering a rectangular coordinate system $Oxyz$ with the origin at the centre of the plate and the axes parallel to the sides of the plate, the locations of the three support points are completely defined by means of the length a, that eventually could be related to the edge l of the plate ($a = 23l/50$, in this case). A concentrated force transversally loads the plate. The location of the force on the surface could be defined by the analysis of the correlation maps.

Fig. 3 reports the mean maps of the correlation coefficients for different shapes of the specimen obtained by considering a suitable number of either isotropic or orthotropic materials. In the first column of the figure the shape of the specimen is schematically represented: by the small squares the location of the support points are emphasized, while the small circle represents the point of the application of the load, which is varied in the numerical simulation in order to evaluate the correlation maps. These maps are reported in the second column, for an isotropic material, and in the third column, for an orthotropic material. Darker is the area of the correlation maps, lower is the degree of correlation and better is the choice for the point of application of the load. As it can be noticed by observing these maps for the orthotropic material an acceptable level for the correlation index is obtained only for the square shaped plate, since for the other shapes the index never assumes values lower than 0.3. Finally it must be pointed out that in the first column, except for the square shaped specimen, the portion of the specimen necessary to apply the procedure is delimited by a dashed closed line.

4. Experimental equipment

The main components of the whole apparatus, which was used for the experimentations described in the present paper, are shown in the sketch of Fig. 4. The apparatus was assembled on an optical bench supported by pneumatic vibration isolators. The light source is a *COHERENT 2W Nd-Yag Model Verdi* operating in single line mode at the wavelength $\lambda = 532$ nm. The laser beam is filtered and expanded and the resulting spherical wavefront is divided by a beamsplitter into two equal intensity beams. The specimen and the

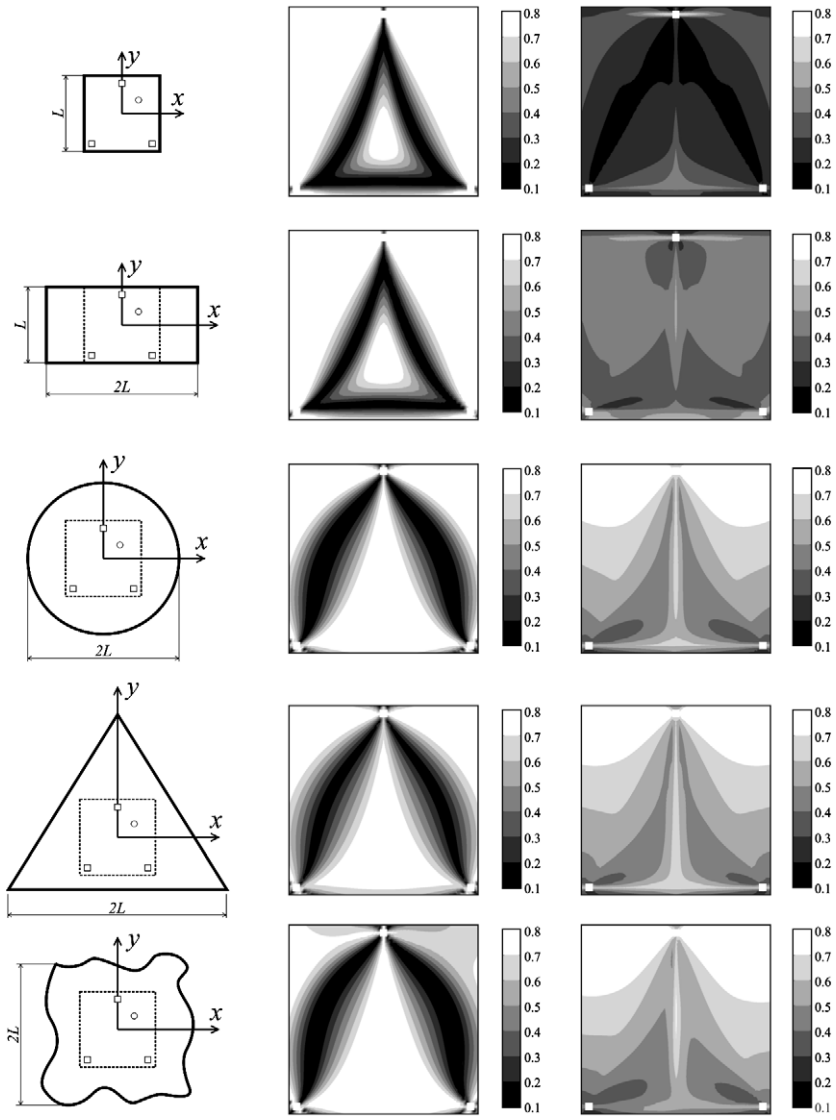

Fig. 3. Maps of the correlation index obtained for a unidirectional laminate.

reference surfaces are horizontal and are illuminated and observed by a 45° oriented mirror with the respect of the propagation direction of the beams. The scattered speckle wavefronts interfere at the image plane of the CCD of the TV camera. The camera is interfaced with a general purpose computer image processing system where the real time fringe patterns are generated by the subtraction of digitalized images. Essentially, the optical setup constitutes a speckle interferometer, based on the Michelson design, for measuring the out-of-plane component of displacements. A picture of the optical layout is reported in Fig. 5.

The specimen is placed in the loading device, as shown in Fig. 6(a), and loaded according to the loading configuration reported in Fig. 2, except from the direction of action of the load and, consequently, of the constraints. The length a was assumed equal to 23 mm and the coordinates of the loading point are $x_F = 5$ mm and $y_F = 3$ mm. The force is applied by a small sphere of 2.3 mm diameter interposed between the lower surface of the specimen and a support plate mounted on a strain-gauged load cell, by which the load is measured with a resolution of 10^{-3} N. Three small spheres of the same diameter support the specimen on the upper surface. These spheres are glued on two parallel rectangular aluminum bars which are rigidly connected each other at their ends by two thin circular bars, as shown in Fig. 6(b). For a correct and repeatable location of the sup-

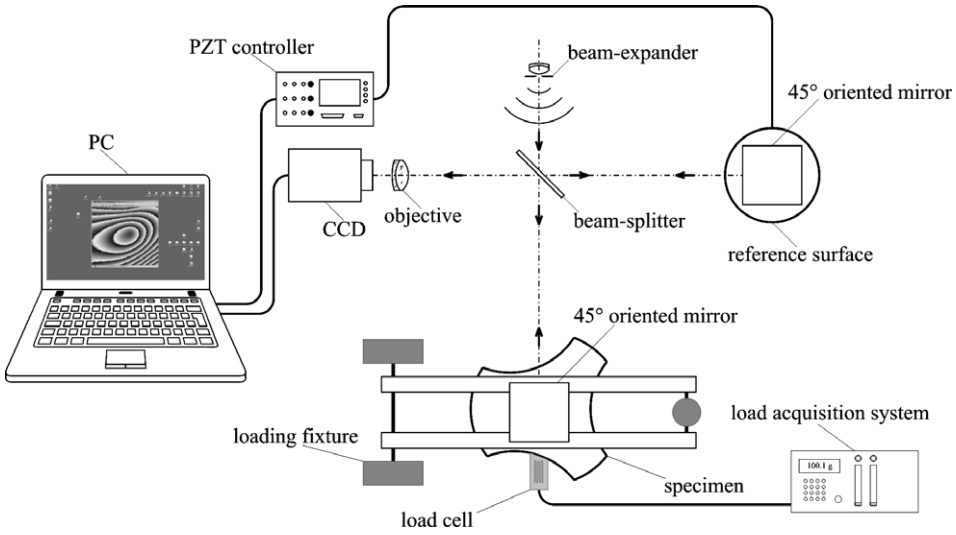

Fig. 4. The experimental apparatus.

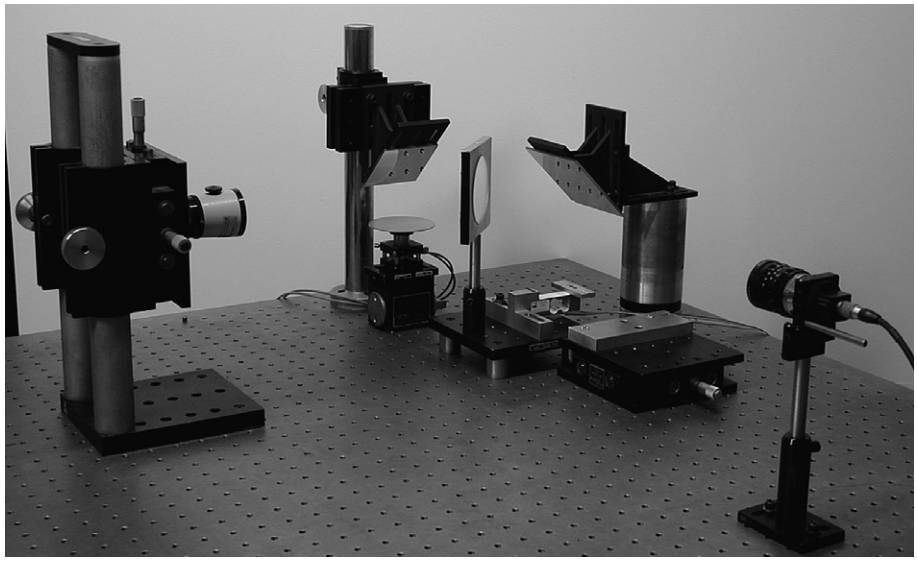

Fig. 5. A picture of the optical set-up.

port points, a suitable kinematic device was properly designed and clamped at one end of the fixture. It allows to remove the fixture and subsequently to reposition it in the same location with interferometric accuracy. The amplitude of the load is controlled by adding sample weights on a plate fixed at the other end of the fixture.

Most of the surface of the specimen (50×44 mm^2) can be observed between the two rectangular bars of the fixture, by the CCD camera. The out-of-plane displacements are measured with a sensitivity equal to $\lambda/2$, which can be increased if the phase variations due to the displacements are measured by applying a phase-shifting procedure. In the present work a four step algorithm was applied by a proper Virtual Instrument (VI) implemented in *National Instruments LabView*™ environment, in order to obtain the phase at each pixel of the visible part of the specimen. The technique requires that four speckle patterns must be captured sequentially in time by the CCD camera. Each frame is shifted by the same amount of phase with respect to the previous one. The phase shift between two successive frames is equal to $\pi/4$; in practice, this change in phase is obtained by translating the reference surface along the vertical axis of an amount equal to $\lambda/8$.

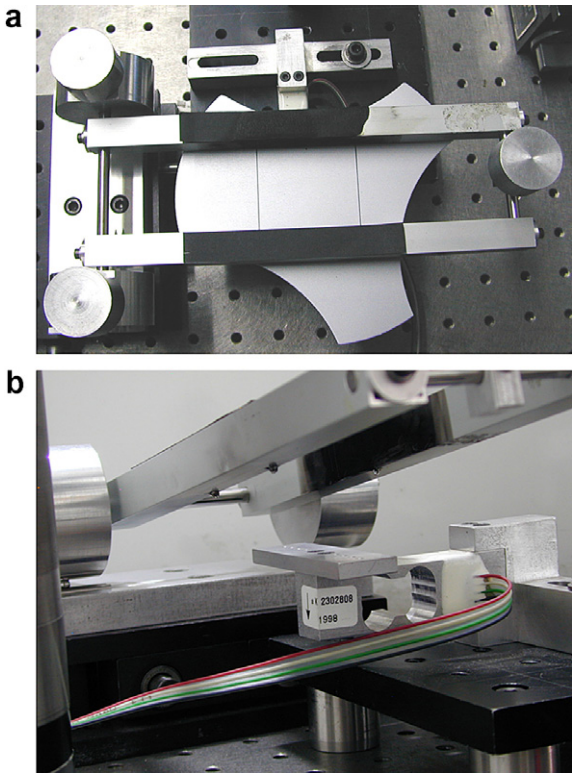

Fig. 6. The loading device: (a) the loading fixture and the generic shaped aluminum plate; (b) the spheres used for reproducing punctual constraints and load.

The light intensity at the kth pixel varies according to the following relation:

$$i_k = i_m + i_a \cos(\delta + \Delta\varphi_k), \tag{2}$$

where i_m, i_a and δ are the mean intensity, the modulation and the phase, respectively, that is the parameters to be determined, while $\Delta\varphi_k$ is the known shift introduced by the phase-shifting procedure. The unknowns can be calculated locally at each pixel of the image by solving the system of linear equations obtained by writing as many equations as the steps (at least three). The phase is then calculated from the light intensity measured at different steps. If a four equispaced $\pi/4$ step algorithm is adopted the phase is calculated according to the following relation:

$$\delta = \arctan\frac{I_4 - I_2}{I_1 - I_3}, \tag{3}$$

where I_i is the light intensity of the ith step. The two arguments *arctan* function was used in order to obtain a phase in the range $[-\pi, \pi]$.

The phase-shifting procedure is entirely performed by a personal computer interfaced by a standard RS232 serial port with the amplifier of a PZT actuator, able to move the reference surface with nanometric accuracy. In fact, by means of the virtual instrument implemented, it is possible to move the actuator and to acquire, by a CCD camera, the speckle intensity patterns scattered from the surface under test. By the virtual instrument is also possible to unwrap the phase maps by proper algorithms able to work in presence of severe noise.

5. The experimental procedure

In order to test the effectiveness and the repeatability of the procedure, this was applied on two specimens of different shape and material. Fig. 7 reports the dimensions and the shapes of the specimens: the square spec-

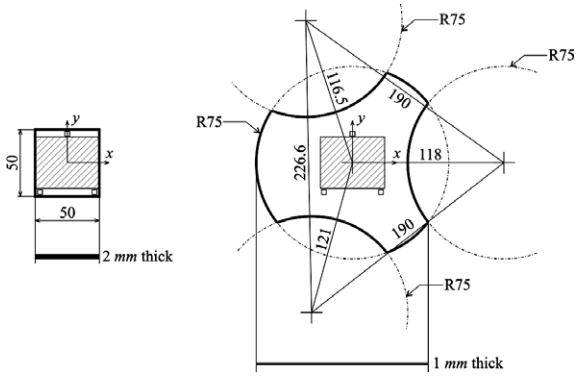

Fig. 7. The geometry of the two specimens.

imen was cut from a unidirectional graphite reinforced PEEK panel; the second specimen was cut from a cold rolled sheet of aluminum alloy 6082-T6. The aluminum specimen was annealed in order to eliminate the strengthening effects of the cold work, according to the technological directives reported by Davis (1998).

Both the specimens were painted, on the observed side, by a non-depolarizing metallic spray paint. The side of the square plate was measured by a standard digital caliper with a resolution equal to 10 μm, while the irregular contours of the second specimen are acquired by a coordinate-measuring machine (CMM with a nominal resolution of 10 μm).

As regards the measurement of the thickness, if the plate has a uniform thickness, a point measurement should be enough. Practically it is always more reliable to determine the mean thickness by averaging over a number of measurements carried out in different points; these measurements were performed by a digital micrometer with a resolution of a 1 μm.

A strain-gauged load cell connected to an HBM amplifier was used to measure the force applied to the plate. To test the repeatability of the experimental tests, different load levels were employed, inside the range of values producing a pattern with a suitable number of fringes (from 30 to 70 and from 70 to 115 g for the aluminum and composite plate, respectively).

A 2D finite element model is developed for each plate, paying attention that a node of the mesh falls in proximity, or eventually exactly at the location, of each support and loading point; the position of these points are traced on the painted side of the specimen before the beginning of the measurement sessions. Then, they are acquired together with the boundary of the plate and the obtained coordinates were used for defining the position of the nodes to be constrained and loaded. Quadratic four node elements (CQUAD4) were used (2500 elements for the square plate and 7600 elements for the generic shape plate) and the effects of the transverse shear deformation was considered in the analysis. Both the meshes are reported in Fig. 8.

For characterizing the material, the specimen must be introduced in the loading fixture by carefully controlling that the three points marked on the upper surface of the plate overlap as accurately as possible with the three support spheres of the loading fixture. If this fact is respected, the real loading and constraining condition coincides with the simulated one. Any definite area on the FEM model corresponds to an area observed by the camera and the measured displacement can be readily associated at each node of the mesh. The lack of alignment between the loading fixture and the plate could imply large errors in the solution.

Because of the loading fixture creates shaded areas on the specimen, the displacements can be retrieved only on a rectangular portion of the surface of the specimen, whose extension is about 50×44 mm^2 (see Fig. 7). This area is focused on approximately 500×500 pixels of the CCD camera.

Typical phase maps are shown in Fig. 9(a). In the optical arrangement, the sensitivity vector was normal to the surface of the specimen, with a module equal to half the wavelength of the light source (532 nm); this means that between two adjacent fringes there is a difference in out-of-plane displacement equal to 266 nm. As it can be seen, fringes are very noisy due to the intrinsic noise of the speckle techniques.

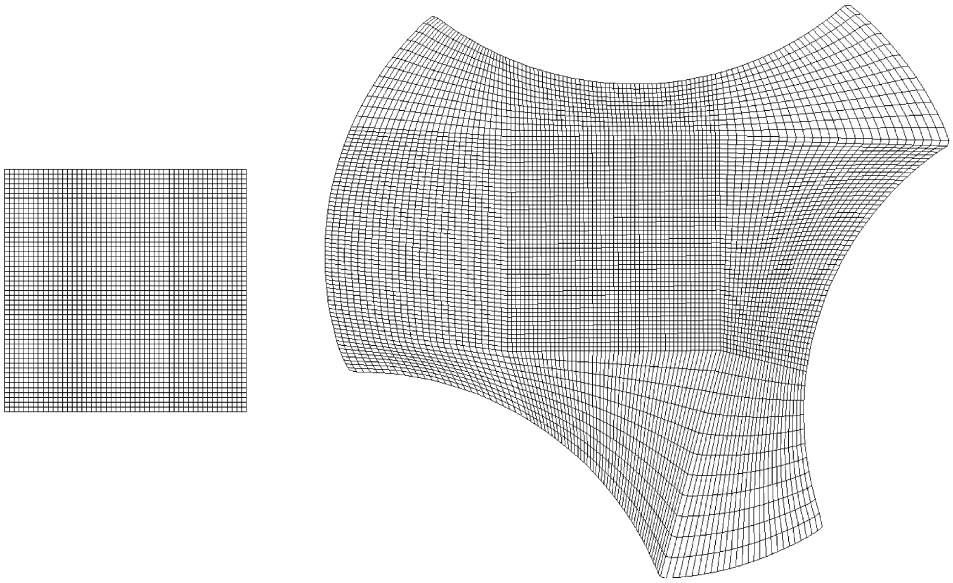

Fig. 8. The meshes created for the numerical analysis of the two specimens.

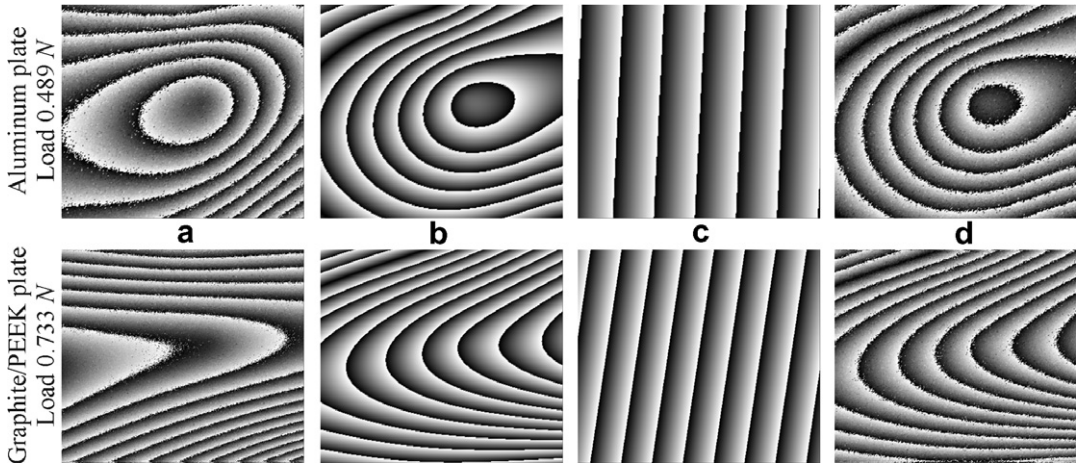

Fig. 9. Experimental and numerical data for the two specimens: (a) experimental data without any manipulation; (b) phase maps obtained by numerical displacement fields; (c) rigid body motion evaluated by the genetic algorithm; (d) experimental data without rigid body motion.

6. Material characterization

Many tests were carried out on both the plates for different load levels with the aim to verify the repeatability and the accuracy of the procedure. Every time, the specimen was removed from the fixture and then repositioned and, for each test, the procedure was applied several times.

The unavoidable rigid body motion of the specimen due to the compliance of the fixture, consisting in a rigid translation along z-axis and two rigid rotations about the x- and y-axis, affects drastically the fringe patterns, leading to an inability to properly identify the elastic constants.

In order to calculate and hence compensate these unwanted effects the fitness of the genetic algorithm was modified. Such a change is based on the fact that difference between the measured $W^{e}(x,y)$ and the numerically calculated $W^{n}(x,y)$ out-of-plane displacements of the plate, except for the measurement noise and the different

elastic constants assumed in the numerical simulations, can be approximated in the space $Oxyz$ by the plane $W(x,y)$ whose equation can be written as:

$$W(x,y) = p_1 x + p_2 y + p_3, \tag{4}$$

where the coefficients (p_1,p_2,p_3) describe analytically the average plane calculated on the experimental data which represents, at the end of the optimization process, the overall rigid body motion. Then, the fitness could be defined as

$$\varphi = (W^{\mathrm{e}} - W^{\mathrm{n}}) - W. \tag{5}$$

Therefore the coefficients p_i can be found by solving the following over-determined system of equations by applying the least mean square method:

$$\begin{bmatrix} 1 & x_1 & y_1 \\ 1 & x_2 & y_2 \\ \vdots & \vdots & \vdots \\ 1 & x_m & y_m \end{bmatrix} \begin{Bmatrix} p_1 \\ p_2 \\ p_3 \end{Bmatrix} = \begin{Bmatrix} w_1^{\mathrm{n}} - w_1^{\mathrm{e}} \\ w_2^{\mathrm{n}} - w_2^{\mathrm{e}} \\ \vdots \\ w_n^{\mathrm{n}} - w_n^{\mathrm{e}} \end{Bmatrix}, \tag{6}$$

where (x_i,y_i) are the coordinates of the ith node. In a compact form, Eq. (6) can be rewritten as:

$$[M]\{p\} = \{w\}, \tag{7}$$

where $[M]$ and $\{w\}$ are the coefficient matrix and the known vector of the over-determined equation system, respectively. By defining the matrix $[C]$ as follows

$$[C] = [M][M]^{+} - [I], \tag{8}$$

in which the superscript $+$ indicates the pseudoinverse of $[M]$, and $[I]$ is the identity matrix. Finally the fitness is evaluated as:

$$\varphi = \|[C]\{w\}\|. \tag{9}$$

Table 1 reports the mean values of 10 tests carried out on both the examined specimens, standard deviation is not reported because the scattering is very low, in fact the standard deviation is less than 1.5% of the mean value.

Since aluminum is an isotropic material, the identification of only two elastic constants is enough. However, in order to investigate the capability of the genetic algorithm to identify the anisotropy of the material, the elastic constants were also evaluated by the four constants algorithm. Nevertheless, the results are also accurate even if four elastic constants are determined. The elastic constants obtained by the proposed technique are compared with those obtained by the authors on the same specimen by a dynamic test based on the measurement of the resonant frequency. The good agreement of the results obtained by the two different approaches confirms the validity of the procedure.

Table 1 reports the results obtained on the composite specimen, these are compared with those obtained by the ASTM standard; also for this material a high repeatability and a good agreement with the results obtained by the other technique can be observed.

Table 1
Comparison between the results obtained by the proposed method and those proposed by different techniques

Material	Method	E_1 (GPa)	E_2 (GPa)	ν_{12}	G_{12} (GPa)
Aluminum	Present (two constants)	71.5	71.5	0.343	
	Dynamic test	72.3	72.3	0.336	
	Present (four constants)	71.0	71.3	0.344	25.5
Graphite/PEEK	Present (four constants)	137.6	10.9	0.271	6.2
	ASTM	134.0	8.9	0.240	7.0

Fig. 9 reports the phase maps for the two types of specimen: in the first row there are the phase maps relative to the aluminum specimen, in the second row those relative to the composite specimen. In particular Fig. 9(a) reports the experimental data without any manipulation, while Fig. 9(b) reports the phase maps which would be obtained if the out-of-plane displacement field matches exactly that obtained numerically. Fig. 9(c) shows the rigid body motion analytically described by Eq. (4) and found by the application of the genetic algorithm when the fitness is calculated by Eq. (9). Finally Fig. 9(d) reports the experimental data obtained by subtracting from the original data the rigid body motion evaluated by the characterization procedure. It must be noticed the high similarity between the numerical data (Fig. 9(b)) and the experimental data without the rigid body motion (Fig. 9(d)).

7. Conclusions

The paper presents a procedure for the elastic characterization of isotropic or orthotropic materials using any-shaped plate specimens subjected to flexural loading configuration. The procedure is based on an optimization procedure which minimizes the difference between numerical displacement field (evaluated by a standard FEM code) and experimental data obtained by a speckle interferometer sensitive to the out-of-plane displacements. The optimization procedure is based on a genetic algorithm able to work directly on the experimental data, without any pre- or post-processing. In the paper, an aluminum generic shaped plate and a unidirectional composite square plate were tested. The results obtained for both the materials have shown a high repeatability and a good agreement with the reference values obtained with other types of techniques.

References

Apalkov, A.A., Odintsev, I.N., Pisarev, V.S., 1999. Implementation of compensation speckle interferometry for high-precision determination of materials mechanical properties. In: Proceedings of SPIE, 3745, pp. 169–179.

Archbold, E., Ennos, A.E., Virdee, M.S., 1978. The deformation of steel bars in a four-point bending machine, measured by holographic interferometry. VDI-Berichte 313, 517–522.

Bruno, L., Furgiuele, F.M., Pagnotta, L., Poggialini, A., 2002a. Determination of elastic constants of anisotropic plates by phase stepping speckle interferometry. Key Engineering Materials 221 (2), 363–373.

Bruno, L., Furgiuele, F.M., Pagnotta, L., Poggialini, A., 2002b. A full-field approach for the elastic characterization of anisotropic materials. Optics and Lasers in Engineering 37 (4), 417–431.

Bruno, L., Felice, G., Pagnotta, L., Poggialini, A., 2006a. A mixed numerical–experimental methodology for determining the elastic constants of orthotropic materials. In: Proceedings of Speckle06. Nîmes, France, 6341, 0J-1-0J-6.

Bruno, L., Pagnotta, L., Poggialini, A., 2006b. Elastic characterization of CVD diamond by static and dynamic measurement. Journal of the European Ceramic Society 26 (12), 2419–2425.

Bruno, L., Poggialini, A., 2005. Elastic characterization of anisotropic materials by speckle interferometry. Experimental Mechanics 45 (3), 205–212.

Cardénas-Garcia, J.F., Ekwaro-Osire, S., Berg, J.M., Wilson, W.H., 2005. Non-linear least-squares solution to the moiré hole method problem in orthotropic materials. Part II: material elastic constants. Experimental Mechanics 45 (4), 314–324.

Carlsson, L.A., Pipes, B.R., 1997. Experimental Characterization of Advanced Composite Materials. Technomic Publishing Company Inc., Lancaster Basel.

Cornu, A., 1869. Méthode optique pour l'etude de la déformation de la surface extériere de solides elastique. Les Comptes Rendus de l'Académie des Science, Paris 69, 333–337.

Davis, J.R., 1998. Metals Handbook, Desk Edition. ASM International, Materials Park, Ohio, USA.

Fällström, K.E., Jonsson, M., 1991. A nondestructive method to determine material properties in anisotropic plates. Polymer Composites 12 (5), 293–305.

Fällström, K.-E., Olofsson, K., Saldner, H.O., Schedin, S., 1996. Dynamic material parameters in an anisotropic plate estimated by phase-stepped holographic interferometry. Optics and Lasers in Engineering 24 (5), 429–454.

Furgiuele, F.M., Muzzupappa, M., Pagnotta, L., 1997. A full-field procedure for evaluating the elastic properties of advanced ceramics. Experimental Mechanics 37 (3), 285–290.

Ganesian, A.R., 1989. Measurement of Poisson's ratio using real-time digital speckle pattern interferometry. Optics and Lasers in Engineering 11, 265–269.

Gascon, F., Salazar, F., 1996. A procedure for calculating through laser speckle interferometry the elastic constants of isotropic materials. Optics Communications 123 (4), 734–742.

Gaul, L., Willner, K., Hurlebaus, S., 1999. Determination of material properties of plates from modal ESPI measurement. Paper presented at the Seventeenth International Modal Analysis Conference. Orlando, FL, 1756–1763.

Genovese, K., Lamberti, L., Pappalettere, C., 2004. A new hybrid technique for in-plane characterization of orthotropic materials. Experimental Mechanics 44 (6), 584–592.

Gibson, R.F., 1994. Principles of Composite Material Mechanics. McGraw-Hill, Singapore.

Grédiac, M., Fourier, N., Paris, P.A., Surrel, Y., 1998. Direct identification of elastic constants of anisotropic plates by modal analysis: experiment and results. Journal of Sound and Vibration 210 (5), 645–659.

Grédiac, M., Paris, P.A., 1996. Direct identification of elastic constants of anisotropic plates by modal analysis: theoretical and numerical aspects. Journal of Sound and Vibration 195 (3), 401–415.

Grédiac, M., Pierron, F., Avril, S., Toussaint, E., 2006. The virtual field method for extracting constitutive parameters from full-field measurements: a review. Strain 42, 233–253.

Grédiac, M., Vautrin, A., 1993. Mechanical characterization of anisotropic plates: experiment and results. European Journal of Mechanics A/Solids 12 (6), 819–838.

Hild, F., Roux, S., 2006. Digital image correlation: from displacement measurement to identification of elastic properties – a review. Strain 42 (2), 69–80.

Jones, R., Bijl, D., 1974. A holographic interferometric study of the end effects associated with the four-point bending technique for measuring Poisson's ratio. Journal of Physics E: Scientific Instruments 7 (5), 357–358.

Lecompte, D., Smits, A., Sol, H., Vantomme, J., Hemelrijck, D.V., 2007. Mixed numerical–experimental technique for orthotropic parameter identification using biaxial tensile tests on cruciform specimens. International Journal of Solids and Structures 44 (5), 1643–1656.

Maletta, C., Pagnotta, L., 2004. On the determination of mechanical properties of composite laminates using genetic algorithms. International Journal of Mechanics and Materials in Design 1, 199–211.

Molimard, J., Riche, R.L., Vautrin, A., Lee, J.R., 2005. Identification of the four orthotropic plate stiffnesses using a single open-hole tensile test. Experimental Mechanics 45 (5), 404–411.

Pagnotta, L., 2006. Determining elastic constants of materials with interferometric techniques. Inverse Problems in Science and Engineering 14 (8), 801–818.

Pagnotta, L., Stigliano, G., 2006. A numerical–experimental approach for identification of material constants of composite laminates by displacement field measurement. WSEAS Transactions on Applied and Theoretical Mechanics 1 (1), 39–46.

Prabhakaran, R., Chermahini, R.G., 1984. Application of the least-squares method to elastic and photoelastic calibration of orthotropic composites. Experimental Mechanics 24 (1), 17–21.

Prabhakaran, R., Saha, M.C., Galloway, T., 2005. Measurement of in-plane elastic moduli of composites with a circular disk specimen and piezoelectric sensors. Polymer Composites 26 (4), 542–551.

Timoshenko, S.P., Goodier, J.N., 1970. Theory of Elasticity. McGraw-Hill Publishing Co., Tokyo.

Wang, W.T., Kam, T.Y., 2000. Material characterization of laminated composite plates via static testing. Composite Structures 50 (4), 347–352.

Wang, Z., Cardénas-Garcia, J.F., Han, B., 2005. Inverse method to determine elastic constants using a circular disk and moiré interferometry. Experimental Mechanics 45 (1), 27–34.

Zhu, J., 1996. Measurement of Poisson's ratio of non-metallic materials by laser holographic interferometry. In: Proceedings of Fourteenth WCNDT. New Delhi, pp. 1481–1484.